Light Metals 2013 *Edited by: Barry Sadler*
TMS (The Minerals, Metals & Materials Society), 2013

MODEL FOR EXCESSIVE CATHODE WEAR BY A "CARBON PUMP" AT THE CELL BOTTOM

Asbjørn Solheim and Kati Tschöpe

SINTEF Materials and Chemistry, P.O. Box 4760 Sluppen, NO-7465 Trondheim, Norway

Keywords: Cathode, wear, aluminium carbide

Abstract

The lifetime of aluminium electrolysis cells is limited by cathode wear, which takes place mainly at the periphery of the cathode. In the present paper it is suggested that excessive wear is due to electrochemical formation and dissociation of aluminium carbide in bath-filled pores within a carbide layer present at the bottom of the cell. The relationship between current and voltage in the pore was established using the Stefan-Maxwell equations on a structure model of the bath, in combination with the calculated reversible voltage and the ohmic voltage drop. A general "wear equation" was derived, describing the relationship between voltage drop along the pore, the thickness and porosity of the carbide layer, and the cryolite ratio. The voltage drop across aluminium carbide layers with different properties is discussed. The model shows that the wear rate will be nearly proportional with the local current density, which is in agreement with practical observations.

Introduction

The service life for aluminium reduction cells is usually limited by excessive wear of the cathode carbon along the periphery of the cell, eventually leading to contact between the metal and the collector bars. The resulting "W" wear pattern in a cross-sectional view of the used cathode [1, 2] is typical for high amperage cells with highly conducting graphitized cathode blocks. Sometimes, even a “double W” pattern can be found [3], and when considering the surface of a used cathode, it seems obvious that more than one mechanism must have been involved. Typical wear rates are in the range from 2 to 6 cm/year [4].

A large number of experimental investigations have been carried out in order to reveal mechanisms and, ultimately, to enable an "accelerated test" for comparing and predicting the performance of different cathode materials [5-10]. However, the different laboratory tests have hitherto not been able to distinguish between different types of carbon. This has lead to the comprehension that the excessive wear associated with modern carbon qualities must be due to some kind of indirect effect, and not related to the cathode quality *per se*. Still, it is fair to say that the reason for the preferential wear along the periphery of the cell is not understood.

One such indirect effect as mentioned above relates to the much higher electrical conductivity in modern carbon types, which leads to extremely non-uniform current density at the cathode surface. The current distribution is related to the ratio between the cross-plane conductivity (perpendicular to the cell bottom) and the in-plane conductivity (along the collector bars) in such a way that the current non-uniformity increases with increasing ratio. A voltage and current distribution in a cathode block made of highly conducting carbon (76000 Sm^{-1}) is shown in Figure 1.

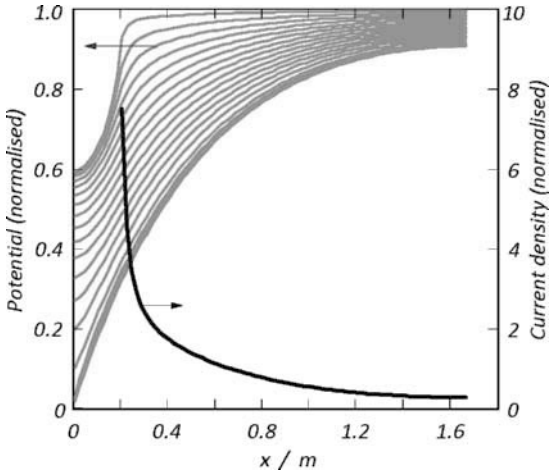

Figure 1. Calculated normalised potentials and normalised current density as a function of the distance along a cathode carbon block from its end to its centre. The potential curves are drawn for each 2 cm from 1 cm below the top of the carbon to 1 cm above the bottom of the collector bar. The sideledge was assumed to extend to x = 0.2 m.

Three different mechanisms for cathode wear were discussed by Solheim [11]; one of them was the possibility of electrochemical formation and dissolution of aluminium carbide within an aluminium carbide layer containing bath-filled pores (carbon pump). The purpose of the present work was to describe that hypothesis in more detail and to quantify some of the parameters involved.

Basic Idea

Electrode and Cell Reactions

Consider a cathode with a layer of aluminium carbide as shown in Figure 2. The carbide layer contains pores filled with electrolyte.

At the cathode (c, bottom of pore), carbide is being formed:

$$\tfrac{3}{4}C(c) + 3Na^+(c) + 3e^- + AlF_3(c) \rightarrow \tfrac{1}{4}Al_4C_3(c) + 3NaF(c) \quad (1)$$

At the anode (a, top of pore), carbide is being oxidized in the exactly opposite reaction,

$$\tfrac{1}{4}Al_4C_3(a) + 3NaF(a) \rightarrow \tfrac{3}{4}C(a) + 3Na^+(a) + 3e^- + AlF_3(a) \quad (2)$$

The current in the electrolyte is assumed to be transported by sodium ions exclusively,

$$3Na^+(a) \rightarrow 3Na^+(c) \qquad (3)$$

The total (cell) reaction becomes the sum of Eqs. (1)-(3),

$$\frac{3}{4}C(c) + 3Na^+(c) + AlF_3(c) + \frac{1}{4}Al_4C_3(a) + 3NaF(a) \rightarrow \frac{3}{4}C(a) + 3Na^+(a) + AlF_3(a) + \frac{1}{4}Al_4C_3(c) + 3NaF(c) \qquad (4)$$

The standard cell voltage for this reaction is zero. Furthermore, the activities of Na^+ and Al_4C_3 are unity at both ends of the pore, and the activity of solid carbon ($a_{C(c)}$) is unity; therefore, the reversible voltage becomes

$$E^{rev} = -\frac{RT}{3F}\ln\frac{a_{NaF(c)}^3 \cdot a_{AlF_3(a)}^3 \cdot a_{C(a)}^{3/4}}{a_{NaF(a)}^3 \cdot a_{AlF_3(c)}^3} \quad [V] \qquad (5)$$

It was assumed that $a_{C(a)}$ is unity as well, although carbon may be dissolved in aluminium with a lower activity. Furthermore, the reactions were assumed to proceed without overvoltages.

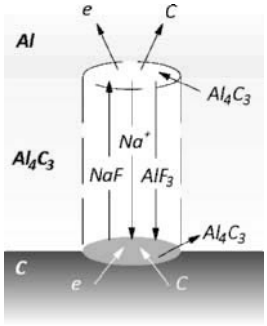

Figure 2. Schematic representation of electrochemical formation and dissolution of aluminium carbide in a pore.

Voltage Drop in the Pore

There will be a voltage drop across the aluminium carbide layer, and this voltage drop must be exactly balanced by the reversible voltage between both ends of the pore and the ohmic voltage drop along the pore,

$$\Delta E = |E^{rev}| + \frac{i_e \delta \tau_b}{\kappa_e} \qquad (6)$$

Here, i_e is the current density inside the pore, δ is the thickness of the carbide layer, τ_b is the tortuosity factor for bath-filled pores, and κ_e is the electrical conductivity of the electrolyte.

Wear Rate

The wear rate at the bottom of the pore (dm/dt) is given by Faraday's law,

$$\frac{dm}{dt} = -\frac{i_e M}{4F} \cdot N \cdot \frac{\pi}{4} d_p^2 \qquad [kgm^{-2}s^{-1}] \qquad (7)$$

where M is the molar weight of carbon, F is Faraday's constant, N is the number of pores per unit cathode area [m^{-2}], and d_p is the pore diameter. The product of pore cross-sectional area and the number of pores is the porosity (φ_b, fraction of carbide layer filled with bath). The average wear rate (change in height) then becomes

$$\frac{dh_{av}}{dt} = \frac{dm}{\rho\, dt} = -\frac{i_e M}{4F\rho} \cdot \varphi_b \quad [ms^{-1}] \qquad (8)$$

The first step is to establish the relationship between voltage and current in the pore.

Model for Current and Voltage in the Pores

Structure Model for Melt

Since the sodium ion carries most of the current, NaF and AlF_3 have to diffuse along the pore. Only the electrolyte components NaF and AlF_3 were considered in the present work. It was assumed that the ideal Temkin model applies for the electrolyte, Na^+ being the only cation, and involving the anions F^-, AlF_6^{3-}, AlF_5^{2-}, AlF_4^-, and $Al_2F_7^-$. The concentration (ion fractions) of the anions can then be determined in the entire composition range by three equilibria between the anions. This is explained in more detail elsewhere [12]. The model fits well with formal activity data in the system NaF-AlF_3 [13], as shown in Figure 3.

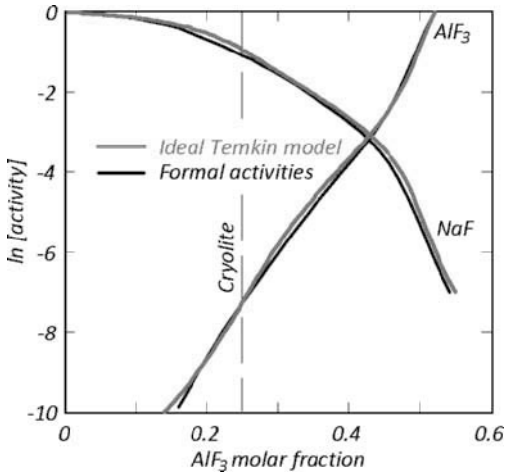

Figure 3. Comparison between ideal Temkin activity model used in the present work and formal activities in the system NaF-AlF_3 [13].

Diffusion in a Multicomponent System

Diffusion in a multi-component system can only be accurately described using the Stefan-Maxwell equation [14]. For numerical solution in a system with five components, this turns into a system of five equations on the form

$$\Delta x_1 = \frac{\Delta y}{\bar{c}_{tot}} \cdot \left(\frac{\bar{x}_1 J_2 - \bar{x}_2 J_1}{D_{12}} + \frac{\bar{x}_1 J_3 - \bar{x}_3 J_1}{D_{13t}} + \frac{\bar{x}_1 J_4 - \bar{x}_4 J_1}{D_{14}} + \frac{\bar{x}_1 J_5 - \bar{x}_5 J_1}{D_{15}} \right) \qquad (10)$$

where x_i is the molar fraction of component i, y is the coordinate in the direction of the pore [m], c_{tot} is the total molar concentration [$molm^{-3}$], D_{ij} (= D_{ji}) is the binary diffusion coefficient for the system i-j [m^2s^{-1}], J is the molar flux [$molm^{-2}s^{-1}$], "Δ" represents

the difference between neighbouring elements, and overlining represents the average of neighbouring elements. With constant molar fluxes, the equation converges rapidly when computing "new" molar fractions using "old" data as input, and then using the "new" data in a new iteration.

In order to fulfil the criterion that the anionic species in the electrolyte should be at equilibrium in any position, the molar fluxes at each point in the calculation domain were varied systematically. The relationships between the individual anion fluxes also depend on the element balance; *e.g.*, the total fluxes of F and Na are zero because they are neither produced nor consumed in the electrode reactions; this is also described elsewhere [12]. The requirement for electro-neutrality was fulfilled by assuming neutral components (*e.g.*, Na_2AlF_5 instead of AlF_5^{2-}; this is possible when Na^+ is the only cation).

The diffusion coefficients D_{ij} in Equation (10) were assumed to be 2×10^{-9} m^2s^{-1} for diffusion pairs containing F^- and 1×10^{-9} m^2s^{-1} for pairs not containing F^-.

Ohmic Resistance

The ohmic voltage drop along the pore (last term in Equation (6)) was calculated using the electrical conductivity equation by Hives *et al.* [15] as a basis; in the system $NaF-AlF_3$ at 960 °C these data can be represented by

$$\kappa_e = 105.9 + 55.33 \cdot r \qquad (11)$$

where r is the NaF/AlF_3 molar ratio. The resistance voltage drop was calculated for each point in the calculation domain; *i.e.*, the change in molar ratio along the pore was taken into account. Since the presence of alumina or calcium fluoride was not taken into account, Equation (11) gives a somewhat too high conductivity. On the other hand, no attempts were made to take into account the electronic conductivity in the dissolved metal-saturated electrolyte, which adds to the ionic conductivity [16].

Reversible Voltage

The reversible cell voltage was calculated from Equation (5). It can be shown that in the $NaF-AlF_3$ system (Na^+ as only cation), the activity of NaF becomes

$$a_{NaF} = \frac{n_{F^-}}{\sum n_-} \qquad (12)$$

where n denotes the number of ions. The activity of AlF_3 becomes

$$a_{AlF_3} = n_{AlF_6^{3-}} \cdot (\sum n_-)^2 / n_{F^-}^3 \qquad (13)$$

Results

A number of calculations were made, using NaF/AlF_3 molar ratios (r) at the top of the pore (anode) ranging from 2.2 to 3.0. Since both the concentration gradients and the ohmic voltage drop depend on the mixed parameter $i_e \cdot \delta \cdot \tau$, this was used as the input parameter in the calculation. An example of concentration gradients along the pore is given in Figure 4.

It turned out that the reversible voltage between the ends of the pore was very large compared to the ohmic voltage drop; the latter was in average 2.2 percent of the reversible voltage. In the case shown in Figure 4, the reversible voltage was 87.4 mV and the ohmic drop was 1.9 mV.

As shown in Figure 5, it turned out that the relationship between the current density, the pore thickness, the tortuosity factor and the total voltage ΔE (sum of ohmic voltage drop and reversible voltage) could be well enough represented by the equation

$$i_e \delta \tau_b = \frac{\Delta E}{0.500 - 0.111r - 0.37\Delta E} \qquad [Am^{-1}] \qquad (14)$$

Upon combination of Equation (8) and (14) and insertion of fixed data (M = 0.012 $kgmol^{-1}$ and F = 96485 $Asmol^{-1}$), we obtain

$$\frac{dh_{av}}{dt} = \frac{98.1 \cdot \varphi \cdot \Delta E}{\rho \delta \tau_b (0.500 - 0.111r - 0.37\Delta E)} \qquad [cm/y] \qquad (15)$$

Equation (15) can be regarded as a "general wear equation". A graphical representation of the equation is shown in Figure 6.

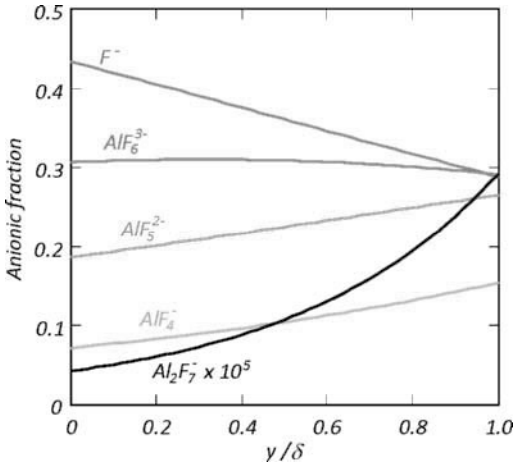

Figure 4. Concentration gradients along the pores. Calculated with r = 2.6 at the top of the pore (y/δ = 1) and $i_e \cdot \delta \cdot \tau = 1$ (see text).

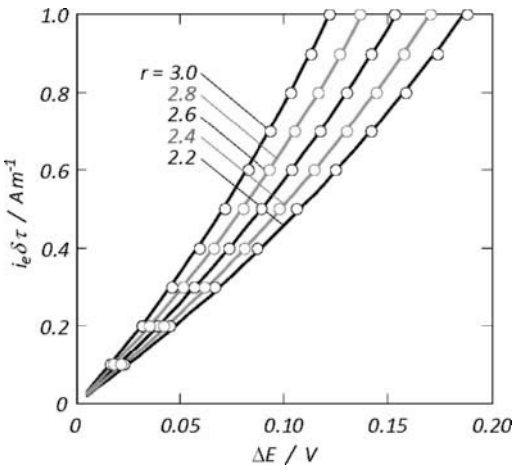

Figure 5. Relationship between the current density, the pore thickness, the tortuosity factor and the total voltage ΔE at different NaF/AlF_3 molar ratios. Symbols – numerical calculations, curves – Equation (14).

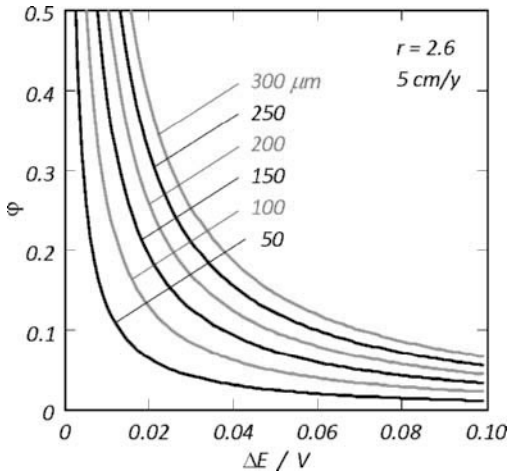

Figure 6. Corresponding values of porosity (φ) of the carbide layer, thickness of the layer, and voltage drop across the layer at a wear rate of 5 cm/y. The density of the carbon was taken to be 1650 kgm^{-3} and the NaF/AlF_3 ratio at the top of the pore was assumed to be 2.6.

Electrical Conduction through the Aluminium Carbide Layer

Homogeneous Aluminium Carbide Layer

In the following, we regard the aluminium carbide layer as consisting of a continuous and homogeneous mixture of aluminium carbide, bath, and aluminium; "homogeneous" meaning that the dimensions of and distances between each phase are smaller than the thickness of the layer.

To obtain a cathode wear rate of 5 cm/y, which is a typical value along the periphery of the cathode, it is probably necessary to have a voltage drop across the carbide layer in the order of 10^{-2}-10^{-1} V at a current density in the order of 10^5 Am^{-2} (see Figures 1 and 6). The corresponding electric conductivity in a 100 μm thick layer must be in the order of 10^2-10^3 Sm^{-1}.

The aluminium carbide itself has an electrical conductivity of about 0.40 Sm^{-1} [17]. The effective conductivity of the bath pores ($\kappa_{p(eff)}$) can be estimated by (see Equation (14))

$$\kappa_{p(eff)} = \frac{i_e \delta \tau_b}{\Delta E} = \frac{1}{0.500 - 0.111 r - 0.37 \Delta E} \approx 5 \mathrm{Sm}^{-1} \quad (17)$$

The above numbers lead to the conclusion that the conductivity of a continuous and homogeneous carbide layer is completely dominated by the conductivity of molten aluminium, which is about 3.6 x 10^5 Sm^{-1} [18]. Still, the effective conductivity will be only 0.03-0.3 % of the conductivity of aluminium, which means that the dimensions of the aluminium must be very (unrealistically?) small to fulfil the "homogeneous" criterion.

Inhomogeneous Aluminium Carbide Layer

An inhomogeneous aluminium carbide layer may be continuous or non-continuous, as illustrated in Figure 7. In both cases, the main part of the current is transported by direct contact between molten aluminium and the carbon surface, while there will be a voltage difference between the top and bottom sides of the carbide layer due to the current shielding effect. Only the non-continuous carbide layer will be treated in the following.

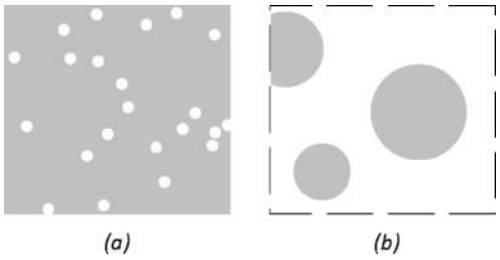

Figure 7. Schematic representation of inhomogeneous aluminium carbide layers at the cathode. a) – continuous layer with aluminium-filled pinholes, b) – non-continuous layer made up of aluminium carbide "islands".

Current Shielding Effect around Aluminium Carbide "Islands"

The current density and potentials around a circular "island" of aluminium carbide, as illustrated in Figure 7 b), were computed. Figure 8 shows local current densities in the vertical direction as computed in COMSOL4.3. As can be observed, the local current density is very high around the edges of the island and smaller above and below the centre of the island. Potential differences are comparably small in the aluminium layer due to the high conductivity. Due to the current shielding effect, the electric potential will be lower directly underneath the island that at the same horizontal level outside the island. Some simplified calculations were made in Excel, as shown in Figure 9. As can be observed; the maximum potential difference between the top and bottom sides of the carbide island increases linearly with the horizontal dimensions. Close to the periphery of the cathode, where the current density will be in the order of 10^5 Am^{-2} in an industrial cell, the potential difference between the top and bottom of the central part of a carbide island with 30 mm diameter layer will be in the order of 0.01 V.

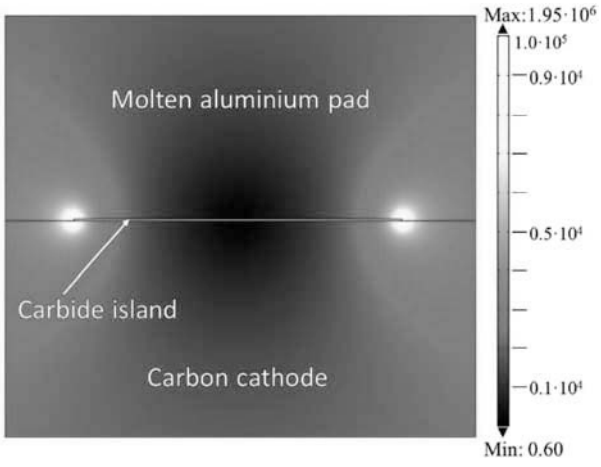

Figure 8. Current density around an aluminium carbide island (2 cm dia, 100 μm thick). The electrical conductivities were assumed to be 3.6 x 10^5 Sm^{-1} for molten aluminium, 8.0 x 10^4 Sm^{-1} for carbon, and 1.0 Sm^{-1} for the carbide layer containing bath-filled pores.

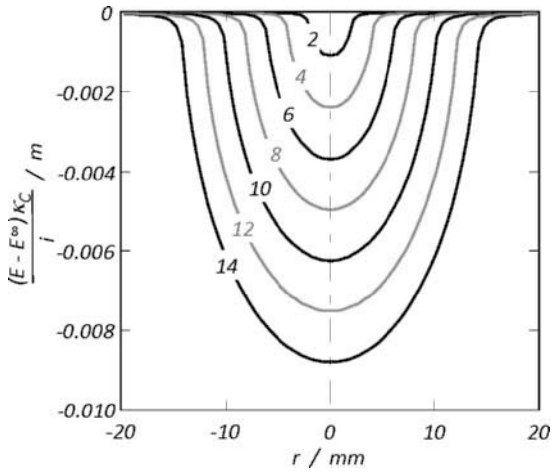

Figure 9. Generalised representation of the potential close to the bottom side of carbide islands with different sizes (radius in mm as given in the figure). The aluminium phase was regarded as being an equipotential region (E^{∞}). κ_C and i are the electrical conductivity of carbon [Sm^{-1}] and the current density outside the island, respectively [Am^{-2}].

Characteristics of the Aluminium Carbide Layer

Obviously, the key point in the hypothesis presented in this paper is the nature of the aluminium carbide layer at the cathode. It is well known from autopsies that most of the cathode carbon surface is covered by aluminium carbide. The carbide is also present in pores inside the cathode [19]. The present authors are of the opinion that the solid aluminium carbide is present at the cathode during the entire cell life.

So far, no experimental or photographic evidence exists that allow estimation of the porosity or the bath content in the carbide layer. Figure 10 shows optical microscope pictures of an approximately 100 μm thick carbide layer in a shut down industrial cell, which indicates that bath filled pores may extend through the carbide layer (best seen in Figure 10 b).

Similar aluminium carbide layers have been observed in laboratory test cells for studying cathode wear. The picture in Figure 11 shows a cross-section of a polarised cathode sample after exposure to bath. The picture shows that there is a region where bath, aluminium, and carbon are mixed, but in this case, there is a dense layer of carbide at the carbon surface, and no pores extending to the carbon can be observed.

A study concerning the appearance and characteristics of the carbide layer is published elsewhere [20], and this is still on-going work.

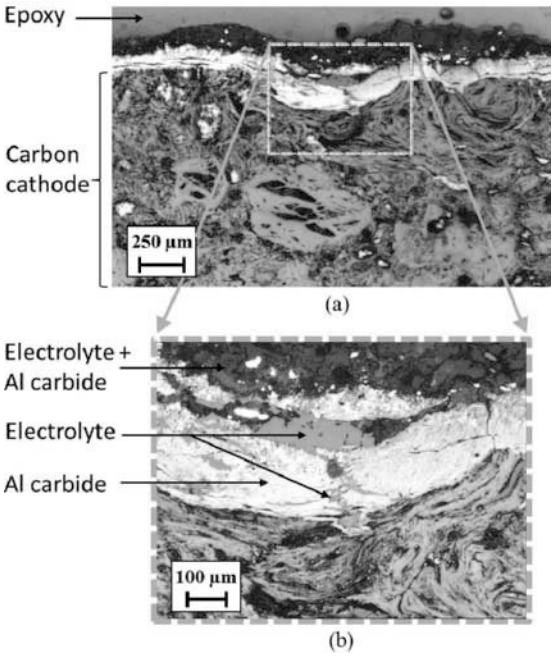

Figure 10. Optical microscope images of the surface region of a carbon cathode block cross section sample taken from an industrial electrolysis cell. The dashed framed boxes represent a magnification showing bath-filled vertical pores in the aluminium carbide layer. The pictures are bright filter images. Pictures by Øyvind Østrem.

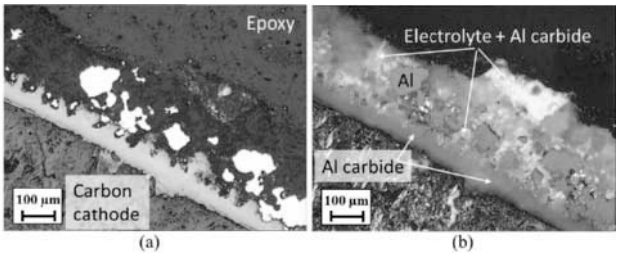

Figure 11. Optical microscope images of the surface region of a carbon cathode cross section sample from a laboratory test cell designed to measure cathode wear rates. Picture a) is the bright filter image and b) is the polarized light image of the same position. The appearance of the carbide and electrolyte layer is similar to industrial cell samples (see Figure 10).

Discussion and Concluding Remarks

In a recent work [10] it was concluded that laboratory tests of different cathode carbon materials performed at the same standardised conditions revealed approximately the same wear rate for all types of material. As mentioned in the introduction, it is probable that the different wear rates and the "W" wear patterns observed in the industry must be due to some kind of indirect effect, and related to the local current density at the cathode. The hypothesis presented in the present paper is the only mechanism suggested so far that provides a direct link between the wear rate and the local current density at the carbon surface. However, there are also other mechanisms related to the local current density that cannot be ruled out. The metal flow velocity will be higher along the periphery of the cathode than at the centre, leading to a higher mass transfer coefficient for dissolution of carbon and/or carbide.

It is also possible that abrasion by alumina particles increases sharply above a certain threshold value for the metal flow velocity.

The present calculations were performed without taking electrochemical overvoltage into consideration. Recent experimental work indicates that the suggested cell reaction (Equation (3)) may in fact not proceed reversibly [19], which implies that the pore current density will be lower than shown in the present work, or that a bigger "carbide island" will be needed to produce the same wear rate.

More work is certainly needed to clarify these issues.

Acknowledgement

The present work was carried out in the project "Durable Materials in Primary Aluminium Production" (DuraMat), financed by the Research Council of Norway, Hydro Primary Metal Technology, Sør-Norge Aluminium, and Elkem Carbon. Permission to publish the results is gratefully acknowledged. Special thanks go to PhD candidate Øyvind Østrem for fruitful discussions, and he also kindly provided the optical microscope pictures taken from an industrial sample.

References

1. M. Sørlie and H.A. Øye, Cathodes in Aluminium Electrolysis, 3r^{d} edition, Aluminium-Verlag, 2010.
2. P. Reny and S.Wilkening, "Graphite Cathode Wear Study at Alouette", Light Metals 2000, pp. 399/405.
3. E. Skybakmoen, S. Rørvik, A. Solheim, K.R. Holm, P. Tiefenbach, and Ø. Østrem, "Measurement of Cathode Surface Wear Profiles by Laser Scanning", Light Metals 2011, pp. 1061/66.
4. D. Lombard, T. Béhérégaray, B. Fève, J.M. Jolas, "Aluminium Pechelney Experience with Graphitized Cathode Blocks", Light Metals 1998, pp. 653/58.
5. S. Wilkening and P. Reny, "Erosion Rate Testing of Graphite Cathode Materials", Light Metals 2004, pp. 597/02.
6. E. Skybakmoen, A.P. Ratvik, A. Solheim, S. Rolseth, and H. Gudbrandsen, "Laboratory Test Methods for Determining the Cathode Wear Mechanism in Aluminium Cells", Light Metals 2007, pp. 815/20.
7. K. Vasshaug, T. Foosnæs, G.M. Haarberg, A.P. Ratvik, E. Skybakmoen, "Wear of Carbon Cathodes in Cryolite-Alumina Melts", Light Metals 2007, pp. 821/26.
8. P.M. Patel, "On the Effect of Formulation and Porosity on Cathode Performance in Modern Aluminium Reduction Cells", PhD thesis, The University of Auckland, New Zealand, 2009.
9. Y. Sato, P. Patel and P. Lavoie, "Erosion Measurements of High Density Cathode Block Samples through Laboratory Electrolysis with Rotation", Light Metals 2010, pp. 817/22.
10. K. Tschöpe, A. Støre, E. Skybakmoen, A. Solheim, T. Grande, and A.P. Ratvik, "Critical Reflections on Laboratory Wear Tests for Ranking Commercial Cathode Materials in Aluminium Cells", Light Metals 2013 (this volume).
11. A. Solheim, "Some Hypotheses Concerning Cathode Wear in Aluminium Electrolysis Cells", MetSoc's Annual Conference of Metallurgists (COM 2011), Montreal, Canada, 2-5 October, 2011 (Proceedings, pp. 135/42).
12. A. Solheim, "Concentration Gradients of Individual Anion Species in the Cathode Boundary Layer of Aluminium Reduction Cells", Light Metals 2012, pp. 665/70.
13. A. Solheim and Å. Sterten,"Activity of Alumina in the System $NaF-AlF_3-Al_2O_3$ at NaF/AlF_3 Molar Ratios Ranging from 1.4 to 3", Light Metals 1999, pp. 445/52.
14. J.T. Welty, C.E. Wicks, and R.E. Wilson, Fundamentals of Momentum, Heat, and Mass Transfer, 3rd edition, John Wiley & Sons, 1984.
15. J. Hives, J. Thonstad, Å. Sterten, and P. Fellner, "Electrical Conductivity of Molten Cryolite-Based Mixtures Obtained with a Tube-Type Cell Made of Pyrolytic Boron Nitride", Light Metals 1994, pp. 187/94.
16. G.M. Haarberg, J. Thonstad, J.J. Egan, R. Oblakowski, and S. Pietrzyk, "Electrical Conductivity Measurements in Cryolite Alumina Melts in the Presence of Aluminium", Light Metals 1996, pp. 221/25.
17. W.R. King and R.C. Dorward, "Electrical Resistivity of Aluminium Carbide at 990-1240 K", *J. Electrochem. Soc.* **132** (2), pp. 388/89 (1985).
18. W.-K. Rhima and T. Ishikawab, "Noncontact Electrical Resistivity Measurement Technique for Molten Metals", *Review of Scientific Instruments* **69** (10), pp. 3628/33 (1998).
19. Øyvind Østrem, NTNU (personal communication, work to be published).
20. B. Novak, K. Tschöpe, A.P. Ratvik and T. Grande, "The Effect of Cryolite on the Formation of Aluminum Carbide at the Carbon Aluminium Interface", Light Metals 2013 (this volume).